THE JOURNAL OF BIOLOGICAL CHEMISTRY
Vol. 274, No. 48, Issue of November 26, pp. 34350–34360, 1999

Printed in U.S.A.

Internalized Epidermal Growth Factor Receptors Participate in the Activation of p21^{ras} in Fibroblasts*

(Received for publication, June 14, 1999, and in revised form, August 20, 1999)

Jason M. Haugh‡§, Alarice C. Huang‡, H. Steven Wiley¶, Alan Wells‖, and Douglas A. Lauffenburger‡ ‡‡§§**

From the ‡Department of Chemical Engineering and the ‡‡Division of Bioengineering & Environmental Health, Massachusetts Institute of Technology, Cambridge, Massachusetts 02139, the ‖Department of Pathology, University of Alabama at Birmingham, Birmingham, Alabama 35294, and the ¶Department of Pathology, University of Utah, Salt Lake City, Utah 84132

Regulated activation of the highly conserved Ras GTPase is a central event in the stimulation of cell proliferation, motility, and differentiation elicited by receptor tyrosine kinases, such as the epidermal growth factor receptor (EGFR). In fibroblasts, this involves formation and membrane localization of Shc·Grb2·Sos complexes, which increases the rate of Ras guanine nucleotide exchange. In order to control Ras-mediated cell responses, this activity is regulated by receptor down-regulation and a feedback loop involving the dual specificity kinase mitogen-activated protein kinase/extracellular signal-regulated kinase kinase (MEK). We investigated the role of EGFR endocytosis in the regulation of Ras activation. Of fundamental interest is whether activated receptors in endosomes can participate in the stimulation of Ras guanine nucleotide exchange, because the constitutive membrane localization of Ras may affect its compartmentalization. By exploiting the differences in postendocytic signaling of two EGFR ligands, epidermal growth factor and transforming growth factor-α, we found that activated EGFR located at the cell surface and in internal compartments contribute equally to the membrane recruitment and tyrosine phosphorylation of Shc in NR6 fibroblasts expressing wild-type EGFR. Importantly, both the rate of Ras-specific guanine nucleotide exchange and the level of Ras-GTP were depressed to near basal values on the time scale of receptor trafficking. Using the selective MEK inhibitor PD098059, we were able to block the feedback desensitization pathway and maintain activation of Ras. Under these conditions, the generation of Ras-GTP was not significantly affected by the subcellular location of activated EGFR. In conjunction with our previous analysis of the phospholipase C pathway in the same cell line, this suggests a selective continuation of specific signaling activities and cessation of others upon receptor endocytosis.

The 170-kDa epidermal growth factor receptor (EGFR)[1] exerts its biological effects in response to binding of specific polypeptide ligands, including epidermal growth factor (EGF) and transforming growth factor-α (TGFα). This leads to activation of the EGFR catalytic tyrosine kinase domain, autophosphorylation of specific residues in its carboxyl terminus, and recruitment and phosphorylation of heterologous signaling proteins (1). The EGFR can also transactivate other members of the erbB receptor family via heterodimerization, enhancing the diversity of potential signaling interactions (2). Overexpression and activating mutations of EGFR and other erbB family members, in conjunction with other permissive mutations, have been widely implicated in transformation and tumorigenesis.

Increased ligand secretion and autocrine signaling through the EGFR can also contribute to uncontrolled cell proliferation. Secretion of TGFα in particular is potently mitogenic, because its dissociation from EGFR after endocytosis promotes receptor recycling; the sparing of receptors from proteolysis allows unabated signaling in the presence of a continuous ligand source (3, 4). In contrast, the interaction of EGF with the receptor persists after internalization by virtue of its relative insensitivity to decreases in pH, yielding continued tyrosine phosphorylation and, later, receptor down-regulation (5–7).

Another broad determinant of cell transformation involves dysregulation of the 21-kDa Ras GTPase, a ubiquitous and highly conserved signaling protein normally converted to the GTP-bound active state in response to stimulation of receptor tyrosine kinases (8, 9). Interruption of Ras GTPase activity prevents hydrolysis of bound GTP to GDP, yielding a constitutively active Ras and unregulated cell proliferation. The biological activity of Ras is completely dependent on posttranslational modifications that lead to its insertion into the plasma membrane. Active Ras aids in the recruitment of other signaling proteins to the membrane via its effector loop, including the Raf serine/threonine kinase, phosphatidylinositol 3-kinase, and activators of the Rho and Rac GTPases (10). Activation of Raf initiates a kinase cascade involving successive activation of the dual specificity mitogen-activated protein kinase and extracellular signal-regulated kinase (Erk) kinase (MEK) and Erk. In fibroblasts, this pathway is required for both cell cycle progression and cell motility, whereas a divergent signaling

* Financial support was provided by the National Science Foundation Biotechnology Program in the Division of Biological & Environmental Systems and NCI, National Institutes of Health. The costs of publication of this article were defrayed in part by the payment of page charges. This article must therefore be hereby marked "*advertisement*" in accordance with 18 U.S.C. Section 1734 solely to indicate this fact.

§ Supported by graduate fellowships from the National Science Foundation and the Merck/Massachusetts Institute of Technology Collaboration.

** Current address: Dept. of Pathology, University of Pittsburgh, Pittsburgh, PA 15261.

§§ To whom correspondence should be addressed. Tel.: 617-252-1629; Fax: 617-258-0204; E-mail: lauffen@mit.edu.

[1] The abbreviations used are: EGFR, epidermal growth factor receptor; EGF, epidermal growth factor; TGFα, transforming growth factor-α; Grb2, growth factor receptor-binding protein 2; Sos, son of sevenless; GEF, guanine nucleotide exchange factor; MEK, mitogen-activated protein kinase and extracellular signal-regulated kinase kinase; PLC, phospholipase C; PIP_2, phosphatidylinositol (4,5)-bisphosphate; SH2, Src homology 2; Erk, extracellular signal-regulated kinase; MEM, minimum essential medium; PIPES, 1,4-piperazinediethanesulfonic acid; WT, wild-type.

pathway involving phospholipase C-γ1 (PLC-γ1) is required for cell motility but is dispensable for mitogenesis (11–13).

Ras is positively modulated by guanine nucleotide exchange factors (GEFs), which accelerate the dissociation of bound nucleotides. This favors the subsequent binding of the more abundant GTP from the cytosol. Stimulation of receptor tyrosine kinases leads to the recruitment of Ras-GEF activity to the membrane, which is sufficient to elicit Ras activation (14, 15). Membrane localization is mediated by adaptor proteins such as Grb2, which uses its SH3 domains to complex with the Ras-GEF Sos and its SH2 domain to interact with phosphotyrosine-containing proteins. For example, the SH2 domain of Grb2 binds the Y1068 minor autophosphorylation site of the EGFR (16). However, the Grb2 SH2 domain has a 5-fold higher affinity for the tyrosine-phosphorylated Shc adaptor protein (17), which binds to autophosphorylated EGFR and erbB-2 using both SH2 and phosphotyrosine-binding domains (18). Given that Shc uses two high affinity phosphotyrosine recognition domains, and also that its preferred binding sites on the EGFR are more extensively phosphorylated than Y1068 *in vivo* (19–21), it is likely that coupling to tyrosine-phosphorylated Shc is the predominant mechanism governing the EGFR-mediated localization of the Grb2·Sos complex (22).

Two distinct mechanisms have been identified that attenuate Ras activation in response to EGFR stimulation. These are desensitization by a MEK-dependent negative feedback loop, which causes disassembly of Shc·Grb2·Sos complexes (23–27), and internalization and down-regulation of the EGFR (28, 29). With regard to the latter mechanism, however, it is unclear when Ras activation is silenced during the intracellular trafficking of the EGFR. Shc can associate with endosomal membranes in response to EGF stimulation, and this Shc pool is efficiently tyrosine phosphorylated in rat liver (30, 31). However, the fact that Ras is a membrane-associated protein suggests that it might be compartmentalized. For example, we previously showed that activated EGFR in internal compartments effectively participate in the tyrosine phosphorylation of PLC-γ1, but not in the hydrolysis of its membrane lipid substrate phosphatidylinositol (4,5)-bisphosphate (32). We therefore endeavored to determine whether active, internalized EGFR could participate in the activation of Ras.

To deconvolute the two modes of Ras regulation, we employed the specific inhibitor PD098059 to block the MEK-dependent feedback loop in NR6 fibroblasts expressing wild-type EGFR, which prolonged Ras-GEF activity on the time scale of receptor internalization. We then quantitatively related the tyrosine phosphorylation of Shc, the coprecipitation of Shc with the EGFR, and the generation of Ras-GTP to the total level of EGFR autophosphorylation. These experiments were performed under conditions that manipulated the relative numbers of EGFR activated at the surface and in internal compartments. We found that receptors in internal compartments were at least as potent as surface receptors in stimulating all of the signaling determinants investigated. Thus, Ras activation mediated by EGFR is attenuated primarily by feedback desensitization rather than by receptor internalization. Coupled with our previous findings that internalized EGFR does not functionally participate in the phospholipase C pathway in the same cell line, these data demonstrate that internalized EGFR can selectively either continue or cease signaling through different pathways.

EXPERIMENTAL PROCEDURES

Cell Culture and Quiescence Protocol—NR6 mouse fibroblasts transfected with wild-type human EGFR (NR6 WT) (11, 33) were cultured using minimum essential medium (MEM)-α/26 mM sodium bicarbonate with 7.5% fetal bovine serum, 2 mM L-glutamine, 1 mM sodium pyruvate, 0.1 mM MEM nonessential amino acids, and the antibiotics penicillin, streptomycin, and G418 (350 μg/ml) as the growth medium. All cell culture reagents were obtained from Life Technologies, Inc. Cells were quiesced at subconfluence using restricted serum conditions without G418 (MEM-α/26 mM sodium bicarbonate with 1% dialyzed fetal bovine serum, 2 mM L-glutamine, 1 mM sodium pyruvate, 0.1 mM MEM nonessential amino acids, and the antibiotics penicillin and streptomycin) for 18–24 h prior to experiments. Experiments were carried out in an air environment using MEM-α/13 mM HEPES (pH 7.4 at 37 °C) with 0.5% dialyzed fetal bovine serum, 2 mM L-glutamine, the antibiotics penicillin and streptomycin, and 1 mg/ml bovine serum albumin as the binding buffer.

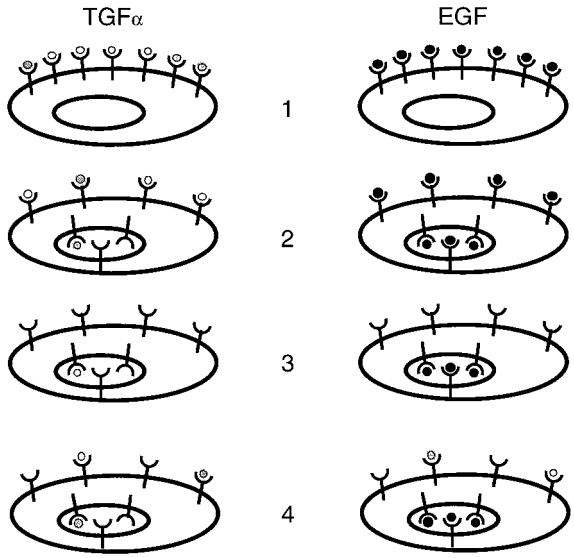

FIG. 1. **Surface titration protocol.** In this procedure, cells are pretreated with a saturating dose (20 nM) of either TGFα (*left*) or EGF (*right*) at 37 °C (*1*). *2,* a sufficient time is allowed for internalization of receptor-ligand complexes; EGF will occupy significantly more internal receptors compared with TGFα. *3.* cells are incubated in ice-cold acid wash (pH 3.0) for 2 min to remove surface-bound ligand; and *4,* cells are returned to 37 °C and pH 7.4 conditions in the presence of various concentrations (0–20 nM) of TGFα. This protocol allows the ligand occupancy of surface and internal EGFR to be manipulated independently.

Pharmacological Inhibitor PD098059—The activation of MEK was selectively blocked using PD098059 (34). The agent, purchased from Calbiochem, was dissolved to a stock concentration of 50 mM in Me_2SO and stored in aliquots at −20 °C. Just before use, an aliquot was warmed to 37 °C and diluted to 50 μM in warm binding buffer. In all cases, cells were preincubated with PD098059 for 60 min at 37 °C before growth factor challenge.

Surface Titration Protocol—This stimulation procedure allows the numbers of activated EGFR at the plasma membrane and in intracellular compartments following endocytosis to be varied independently, as described previously (32) and illustrated in Fig. 1. Briefly, after preincubation with either PD098059 or vehicle only (0.1% Me_2SO), mouse EGF (Life Technologies) or human TGFα (Peprotech) was added to 20 nM in the same medium for 20 min. Cells were then washed once with ice-cold WHIPS buffer (20 mM HEPES, 130 mM NaCl, 5 mM KCl, 0.5 mM $MgCl_2$, 1 mM $CaCl_2$, 1 mg/ml polyvinylpyrrolidone, pH 7.4) and incubated in an acid wash (50 mM glycine-HCl, 100 mM NaCl, 1 mg/ml polyvinylpyrrolidone, pH 3.0) on ice for 2 min. By 1 min, this treatment is equally efficient in dissociating EGF and TGFα from surface EGFR of NR6 cells. After another wash with ice-cold WHIPS, cells were reequilibrated for 5 min in 37 °C binding buffer containing various concentrations of TGFα (0–20 nM) in the continued presence of either PD098059 or Me_2SO only. Thus, a constant level of internal receptor activation, depending only on whether cells were pretreated with EGF or TGFα, is titrated with various levels of surface receptor activation following the acid wash.

EGFR Autophosphorylation—Tyrosine phosphorylation of the EGFR was assessed using a quantitative sandwich enzyme-linked immunosorbent assay. High-binding 96-well plates (Corning) were precoated with 10 μg/ml anti-EGFR monoclonal antibody 225 in PBS and then with blocking buffer (10% horse serum/0.05% Triton X-100 in PBS), at room temperature. After various treatments, cells were washed with ice-cold PBS supplemented with 1 mM sodium orthovanadate; scraped into

ice-cold lysis buffer (50 mM HEPES, pH 7.0, 150 mM NaCl, 1% Triton X-100, 10% glycerol) supplemented with 1 mM sodium orthovanadate, 10 mM sodium pyrophosphate, 1 mM EGTA, 4 mM sodium iodoacetate, and 10 μg/ml each of aprotinin, leupeptin, chymostatin, and pepstatin A; transferred to an Eppendorf tube; and incubated on ice for 20 min. Lysates were clarified by centrifugation, diluted to various extents in blocking buffer supplemented with 1 mM sodium orthovanadate, and incubated in the antibody-coated wells for 1 h at 37 °C. The amount of associated phosphotyrosine was determined using alkaline phosphatase-conjugated RC20 anti-phosphotyrosine antibody (Transduction Laboratories) and *p*-nitrophenyl phosphate (Sigma) substrate as described previously (32).

Shc Tyrosine Phosphorylation and Coprecipitation with the EGFR—1% Triton X-100 cell lysates were generated as detailed above. Immunoprecipitations were performed using 5 μg of PY20 anti-phosphotyrosine antibody or anti-EGFR antibody 225 precoupled to protein G-Sepharose, or 5 μg of anti-Shc polyclonal antibodies (Transduction Laboratories) precoupled to protein A-Sepharose. The antibody-coupled beads were incubated with equivalent total cellular protein amounts (determined by Micro BCA assay using bovine serum albumin as the standard; Pierce) or with equivalent lysate volumes at 4 °C for 60–90 min. For the latter case, employed to enhance recovery of coprecipitating proteins, total protein amounts were determined subsequently. The Sepharose beads were washed five times with ice-cold lysis buffer supplemented with 1 mM sodium orthovanadate, and the residual liquid was removed with a syringe. Precipitated proteins were subjected to SDS-polyacrylamide gel electrophoresis on 10% acrylamide gels and transferred to polyvinylidene difluoride membranes. Membranes were immunoblotted using anti-Shc polyclonal antibodies (Transduction Laboratories) and horseradish peroxidase-conjugated anti-rabbit IgG, or with horseradish peroxidase-conjugated RC20 anti-phosphotyrosine antibody. Protein bands were detected and quantified using SuperSignal Ultra detection reagent (Pierce) and a Bio-Rad chemiluminescence screen and molecular imager, and band intensities were normalized to total cell protein amounts.

Ras Immunoprecipitation and Elution of Guanine Nucleotides—After various treatments, cells were lysed in ice-cold Ras extraction buffer (50 mM Tris-HCl, pH 7.4, 150 mM NaCl, 1% Nonidet P-40, 20 mM $MgCl_2$) supplemented with 1 mM phenylmethylsulfonyl fluoride and 10 μg/ml each of aprotinin, leupeptin, chymostatin, and pepstatin A. After incubation on ice for 20 min, each lysate was clarified; transferred to a new tube; adjusted to 500 mM NaCl, 0.5% deoxycholate, and 0.05% SDS; and subjected to 2 h of immunoprecipitation at 4 °C using 3 μg of Y13-259 anti-Ras monoclonal antibody precoupled with 30 μg of rabbit anti-rat IgG and 10 μl of protein A-Sepharose beads. The immune complexes were washed 10 times with high salt buffer (50 mM Tris HCl, pH 7.4, 500 mM NaCl, 10 mM $MgCl_2$, 0.1% Triton X-100, and 0.005% SDS) and 3 times with 20 mM Tris phosphate, pH 7.8, and residual liquid was removed using a syringe. The beads of each sample were resuspended in 40 μl of elution buffer (5 mM Tris phosphate, pH 7.8, 2 mM EDTA, 2 mM dithiothreitol), boiled for 3 min, cooled briefly on ice, and pelleted for 5 min at 16,000 $\times$ *g*. The supernatants, containing guanine nucleotides dissociated from the immunoprecipitated Ras, were collected and either analyzed immediately or stored at −80 °C.

Ras Guanine Nucleotide Exchange—Ras-GEF activity was measured by permeabilization of cells with digitonin and uptake of [α-^{32}P]GTP by Ras (35). Cells quiesced in 150-mm plates were washed once with ice-cold permeabilization buffer (10 mM PIPES-KOH, pH 7.4, 120 mM KCl, 30 mM NaCl, 5 mM $MgCl_2$, 0.8 mM EGTA, 0.64 mM $CaCl_2$, and 1 mM ATP) after various treatments and then incubated with 0.5 ml of permabilization buffer supplemented with freshly added 0.1% digitonin (Roche Molecular Biochemicals) and 25 μCi of [α-^{32}P]GTP (NEN Life Science Products) for 2 min at 37 °C. The liquid was aspirated carefully. Cells were lysed, Ras was immunoprecipitated, and nucleotides were eluted as described above, except that 1 mM ATP and 100 μM each of GTP and GDP were included in the extraction buffer, and clarified lysates were precleared using 50 μl of protein A-Sepharose beads for 5 min at 4 °C. Radioactivity eluted from Ras was quantified by liquid scintillation counting.

GTP and GDP Determination—The extent of Ras activation was determined using quantitative assays developed by Scheele *et al.* (36) that independently assess absolute, fmol amounts of GDP and GTP eluted from Ras immunoprecipitates. Ras was immunoprecipitated from cell lysates, and guanine nucleotides were eluted, as described above. The absolute amount of GTP eluted from immunoprecipitated Ras was determined using a kinetic assay, in which GTP is converted to ATP by nucleoside 5′-diphosphate kinase (NDP kinase) in the presence of excess ADP, and ATP is consumed by the highly sensitive firefly luciferase reaction to produce light (36). The reaction, monitored in a photon-counting luminometer (MGM Instruments), contained equal volumes of eluate sample and an enzyme mixture. The latter consisted of ATP assay mix (Sigma; FL-AAM), supplemented with 1 μM ADP (purified by high pressure liquid chromatography to remove ATP contamination) and 1 unit/ml NDP kinase (Sigma) (purified by dialysis). Levels of GTP in samples were determined by integrating photon counts over 10 min and subtracting counts obtained for a control sample in which Y13-259 anti-Ras antibody was omitted from the immunoprecipitation. The amount of GDP was determined by equilibrium conversion of GDP and radioactive ATP to ADP and radioactive GTP using NDP kinase, with subsequent separation of GTP and ATP by TLC. 5 μl of sample was reacted with 250 fmol of unlabeled ATP, 0.1 μCi of [γ-^{32}P]ATP (purified by TLC), and 25 milliunits of NDP kinase in the presence of 50 mM Tris-HCl, pH 7.4, and 10 mM $MgCl_2$ (15 μl total reaction volume) for 90 min at 37 °C. 10 μl of each reaction mixture was spotted onto a plastic-backed cellulose TLC plate (Baker). After being developed as in (36), the plate was exposed to a Bio-Rad phosphor screen overnight for subsequent imaging and analysis.

RESULTS

Feedback Desensitization of Ras Guanine Nucleotide Exchange—Activation of Ras is transient in fibroblasts, achieving a maximum after only 2 min or so of EGFR stimulation (28, 37). On the other hand, trafficking of the EGFR between the surface and intracellular compartments requires about 20 min to reach a quasi-steady state in NR6 WT cells (32, 33). Although receptor internalization may play a role in the deactivation of Ras, it is also known that a MEK-dependent feedback loop, acting downstream of receptor activation and upstream of Ras activation, is a potent regulatory mechanism in this pathway (23–27).

In order to deconvolute the potential contributions of the MEK-dependent negative feedback loop and EGFR trafficking to Ras deactivation in NR6 WT fibroblasts, the pharmacological agent PD098059 (34) was employed to block the former mechanism; this inhibitor selectively binds to MEK and prevents its activation by Raf. PD098059 affects biological responses of NR6 WT cells to EGF with an apparent IC_{50} of approximately 10 μM (13). The agent was therefore expected to prolong activation of Ras, as it does in other fibroblast lines. To confirm this, an assay that assesses Ras guanine nucleotide exchange was used, as this activity is the proposed target of MEK-dependent desensitization. NR6 WT cells were permeabilized with digitonin, in the presence of [α-^{32}P]GTP, and Ras-associated radioactivity was immunoprecipitated. After 2 min of maximal (20 nM) EGF stimulation, a 3.6-fold increase in Ras-specific GNP exchange was observed (after subtracting nonspecific cpm) (Fig. 2). This is in agreement with translocation of exchange activity (measured *in vitro*) to the plasma membrane in NR6 WT, which is elevated about 3-fold after 2 min stimulation (38). After 20 min of EGF stimulation, GNP exchange activity decreased to nearly the basal level, consistent with the desensitization of Ras activation seen in other fibroblast lines. However, treatment with PD098059 led to maintenance of elevated Ras-GNP exchange activity (2.8-fold above basal) after 20 min (Fig. 2). PD098059 had no effect on the basal activity (data not shown). Thus, on the time scale of EGFR trafficking, Ras activation is desensitized in a MEK-dependent manner in NR6 WT cells.

Compartmentalization and Desensitization of EGFR Autophosphorylation—We previously demonstrated that the EGFR remains maximally tyrosine-phosphorylated after internalization of EGF, but not TGFα, in NR6 WT cells (32). This was shown using both pH 3 dissociation of surface-bound ligand and clearance of surface-biotinylated proteins from anti-EGFR immunoprecipitates. The difference in internal receptor activation was not surprising, because TGFα exhibits a much lower affinity than EGF for the EGFR at the acidic pH typically found in sorting endosomes (6) and is expected to dissociate from internalized receptors. Exploiting the difference in pH-depend-

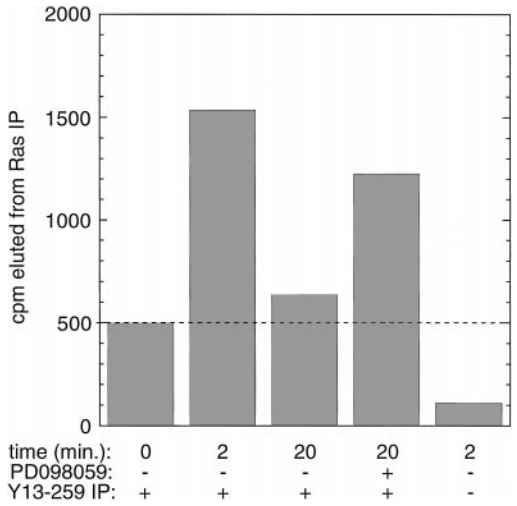

FIG. 2. **MEK-dependent desensitization of Ras guanine nucleotide exchange.** To confirm that inhibition of MEK activation could prolong Ras guanine nucleotide exchange activity *in vivo*, NR6 WT fibroblasts were pretreated with 50 μM PD098059 or vehicle only for 60 min, and then challenged with 20 nM EGF for the times indicated. The cells were permeabilized with digitonin in the presence of [α-^{32}P]GTP, as described under "Experimental Procedures." Ras was immunoprecipitated using Y13-259 monoclonal antibodies, and the associated radioactivity reflects the rate of Ras GNP exchange. Nonspecific binding was assessed by omitting the primary antibody from the immunoprecipitation (Y13-259 −).

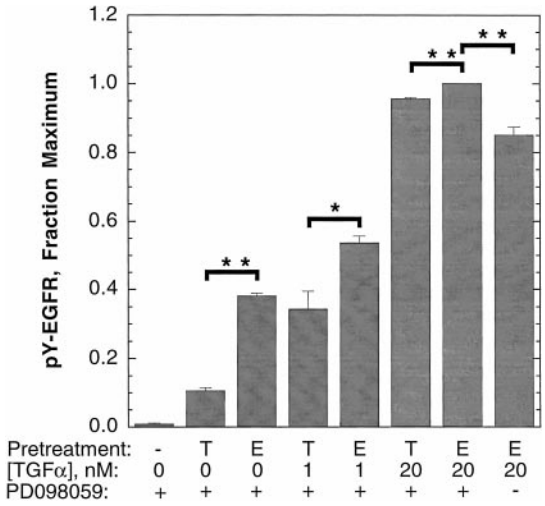

FIG. 3. **Compartmentalization of activated EGFR.** After preincubation with PD098059 or vehicle only, cells were allowed to internalize TGFα (*T*) or EGF (*E*) for 20 min. Surface-bound ligand was removed by acid washing, and the indicated concentration of TGFα was subsequently added for 5 min before cell lysis (surface titration protocol). The levels of tyrosine-phosphorylated EGFR in cell extracts were determined using a sandwich enzyme-linked immunosorbent assay, as described under "Experimental Procedures." Values are mean ± S.E., n = 3; *, Student's t test, $p < 0.05$; **, Student's t test, $p < 0.01$.

ent binding properties between the two ligands, we devised a method for varying the levels of activated EGFR at the surface and in internal compartments independently (32). This surface titration protocol is described under "Experimental Procedures" and illustrated in Fig. 1. In the absence of PD098059 treatment, EGF-pretreated cells yield higher levels of tyrosine-phosphorylated EGFR than TGFα-pretreated cells for the same chase conditions, and this protocol was used effectively to investigate compartmentalization of the PLC-γ1 signaling pathway (32).

To assess whether activation of Ras is compartmentalized, the same experimental design was employed, in conjunction with inhibition of Ras-GEF desensitization. When the surface titration protocol was performed on PD098059-treated NR6 WT cells, EGF-pretreated cells again yielded higher levels of EGFR activation than TGFα-pretreated cells for each chase concentration of TGFα (Fig. 3). However, for the 20 nM TGFα chase condition, the difference in total Tyr(P)-EGFR between EGF- and TGFα-pretreated cells, although still statistically significant, was diminished relative to that seen without PD098059; the ratio of TGFα/EGF pretreated values is 0.95 with PD098059 and 0.84 without (32). We attribute this to changes in feedback mechanisms regulating EGFR kinase and/or tyrosine phosphatase activities (39) rather than to a loss of internal EGFR phosphorylation relative to the surface. That such mechanisms are affected by MEK inhibition is evidenced by comparing EGF-internalized cells chased with 20 nM TGFα that were preincubated with either PD098059 or vehicle only. PD098059 treatment yielded an 18% increase in total EGFR tyrosine phosphorylation (Fig. 3). Also, PD098059 treatment does not drastically affect the surface:internal ratio of cell-associated ligand after a 20-min challenge with 20 nM ^{125}I-EGF; the percentage of internal was 37% for both no treatment and 0.1% Me_2SO preincubation, and 32% for PD098059 preincubation. This is expected because the specific pathway of EGFR internalization (40) is significantly saturated under these stimulation conditions (data not shown).

Internalization of the EGFR Does Not Affect Tyrosine Phosphorylation of Shc—Tyrosine phosphorylation of Shc, which affects the ability of Shc to couple Grb2·Sos complexes with Ras activation, was measured in detergent lysates of NR6 WT cells by immunoprecipitation and immunoblotting. We confirmed that the detected band intensity is proportional to the amount of lysate subjected to the procedure (Fig. 4), demonstrating that our assay is quantitative.

To test whether compartmentalization of activated EGFR affects the ability of the receptor to stimulate tyrosine phosphorylation of Shc, cell lysates were generated for the same surface titration conditions used in Fig. 3. In two separate experiments, the levels of tyrosine-phosphorylated Shc were determined by subjecting equal protein amounts to immunoprecipitation with anti-phosphotyrosine antibodies and immunoblotting with anti-Shc antibodies, as in Fig. 4. A representative immunoblot is shown in Fig. 5*A*, demonstrating that all three Shc isoforms were detected. Because binding of Grb2 or other proteins to tyrosine-phosphorylated Shc could prevent binding of anti-phosphotyrosine antibodies during immunoprecipitation, the levels of tyrosine-phosphorylated Shc were also determined once by immunoprecipitating with anti-Shc antibodies and immunoblotting with anti-phosphotyrosine antibodies. This yielded the same results for phosphorylation of the 46- and 52-kDa isoforms, but the background was too high to allow quantitation of the much less abundant 66-kDa isoform (data not shown).

Because Shc is maximally phosphorylated by 1 min of EGF stimulation in NR6 WT cells (38), it was reasoned that Tyr(P)-Shc is in equilibrium with activation of EGFR on the time scale of our experiments. The normalized level of tyrosine-phosphorylated Shc, averaged over all experiments, was plotted *versus* EGFR-phosphotyrosine for each experimental condition (Fig. 5*B*). Phosphorylation of the 66-kDa Shc isoform, which has been reported to antagonize signaling through the 46- and 52-kDa isoforms (41), is shown as a separate curve. If a signaling readout, such as Shc phosphorylation, does not depend on the location of activated receptors, then all points would lie on the same curve when the data are plotted in this manner. For the surface titration protocol, EGF- and TGFα-pretreated cells differ greatly with respect to activation of internal EGFR, yet

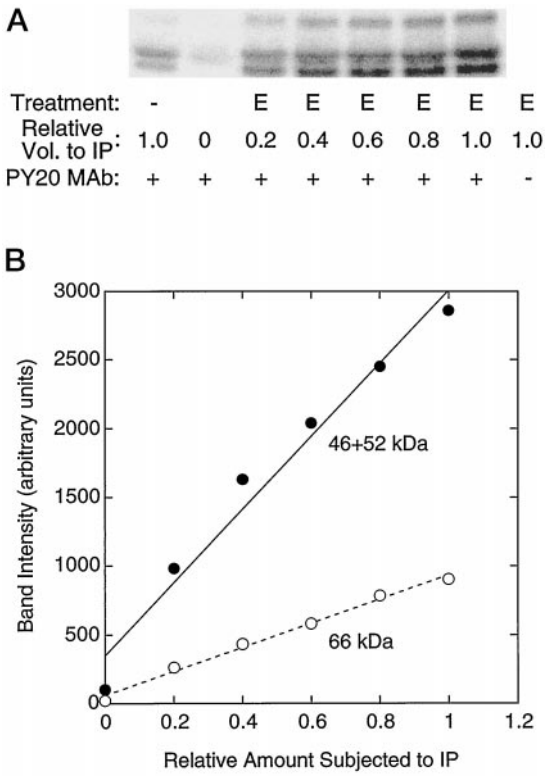

FIG. 4. **Quantitative immunoblotting of tyrosine-phosphorylated Shc.** Cells were either unstimulated (−) or treated with EGF (*E*) and lysed. Tyrosine-phosphorylated proteins were immunoprecipitated from the indicated relative volumes of lysate using PY20 monoclonal antibodies, separated by SDS-polyacrylamide gel electrophoresis, and subjected to immunoblotting with anti-Shc polyclonal antibodies. *A,* chemiluminescent bands were visualized using a molecular imager. *B,* analysis of the detected bands for EGF-treated cells confirmed that the assay is quantitative.

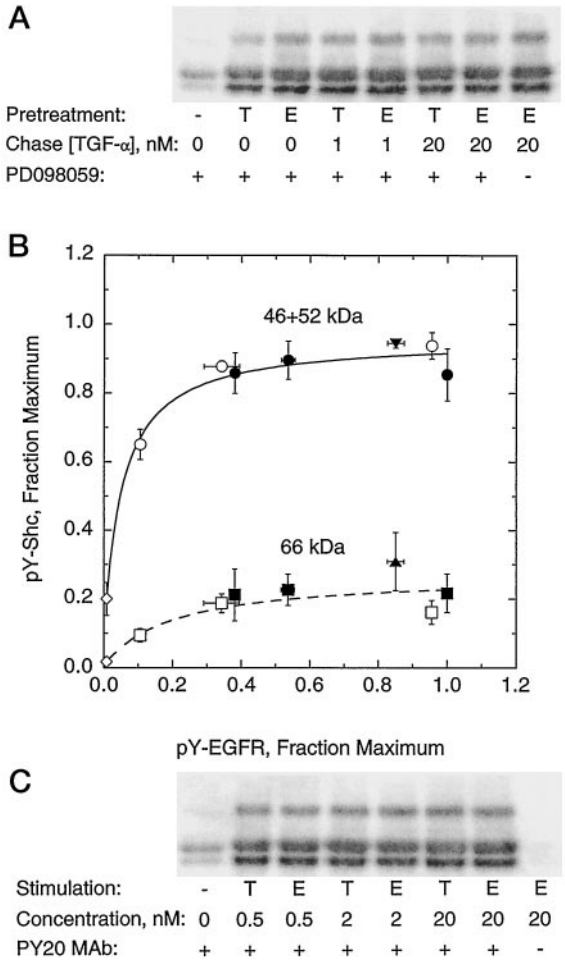

FIG. 5. **Tyrosine phosphorylation of Shc elicited by surface and internal EGFR.** After preincubation with PD098059 or vehicle only, cells were allowed to internalize TGFα (*T*) or EGF (*E*) for 20 min. Surface-bound ligand was removed by acid washing, and the indicated concentration of TGFα was subsequently added for 5 min before cell lysis (surface titration protocol). The levels of tyrosine-phosphorylated Shc were determined by phosphotyrosine immunoprecipitation/Shc immunoblotting ($n = 2$) (*A,* representative blot) or Shc immunoprecipitation/phosphotyrosine immunoblotting ($n = 1$). *B,* relationship to receptor activation. *x* axis values are from Fig. 3 (mean ± S.E.), and *y* axis values are mean ± S.E. (46 + 52 kDa, $n = 3$; 66 kDa, $n = 2$). ◇, no ligand before or after acid wash. ○ and □, pretreatment with TGFα; all *closed symbols,* pretreatment with EGF. ▼ and ▲, preincubation with 0.1% Me_2SO only; ● and ■, preincubation with 50 μM PD098059. *C,* TGFα (*T*) and EGF (*E*) dose responses. Cells were treated with the indicated concentration of ligand for 20 min, and the levels of Tyr(P)-Shc in cell lysates were assayed as in *A*.

points for both ligand pretreatments fall on the same curve in Fig. 5*B*. This is consistent with activated EGFR at the plasma membrane and in endosomes contributing equally to Shc phosphorylation. Also, treatment with PD098059 did not affect tyrosine phosphorylation of the 46- and 52-kDa Shc isoforms. This is consistent with the proposed MEK-dependent mechanism of Ras exchange activity desensitization, which acts downstream of Shc phosphorylation by tyrosine kinases.

The relationship between Tyr(P)-Shc and Tyr(P)-EGFR is saturable, as Shc phosphorylation was insensitive to receptor autophosphorylation when more than one-third of the EGFR was activated (Fig. 5*B*). This was not due to phosphorylation of all cellular Shc molecules, as only about 10% of cellular Shc could be immunoprecipitated by PY20 antibodies (data not shown). To exclude the possibility that the observed relationship was an artifact of slow Shc dephosphorylation following the acid wash, a 20-min dose response with 0.5–20 nM EGF or TGFα was performed. Treatment with 0.5 nM TGFα for 20-min yields approximately 18% maximal EGFR autophosphorylation (32). In this range, Shc phosphorylation was again insensitive to receptor activation (Fig. 5*C*), in accord with a dose response performed by others (38). Shc phosphorylation was the same for EGF- and TGFα-treated cells.

Internalization of the EGFR Does Not Affect Its Ability to Complex with Shc—In addition to tyrosine phosphorylation of Shc, recruitment of Shc to cellular membranes is expected to be important for its role in activating Ras. This localization could be mediated by direct binding of Shc to autophosphorylated EGFR, or by binding to erbB-2 transactivated by heterodimerization with EGFR (42), which may be affected by internalization of the EGFR. The extent of coprecipitation between EGFR and Shc was therefore quantified for the same surface titration conditions used in Figs. 3 and 5.

In two separate experiments, lysates were subjected to EGFR immmunoprecipitation and immunoblotting with anti-Shc antibodies. A representative immunoblot is shown in Fig. 6*A*. All three Shc isoforms were again detected; however, the 66-kDa bands were too weak to be accurately quantified when 500 μg of lysate protein or less was subjected to immunoprecipitation. In a separate experiment, EGFR/Shc complexes were immunoprecipitated with anti-Shc polyclonal antibodies and detected by immunoblotting with anti-phosphotyrosine antibodies, yielding similar results (data not shown). In the 170–185-kDa range, the EGFR and the related orphan receptor erbB-2 are the only known tyrosine-phosphorylated proteins that bind Shc.

The quantitative relationship between the normalized level

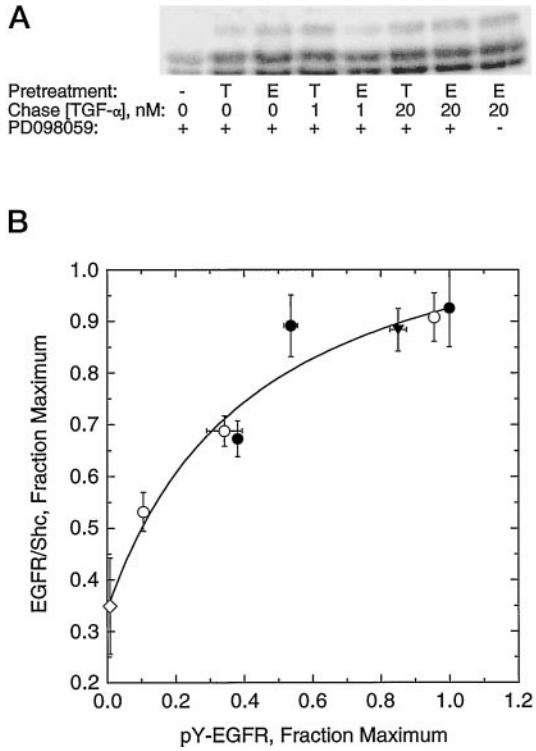

FIG. 6. **Coprecipitation of Shc with surface and internal EGFR.** Cells were treated according to the surface titration protocol, and the extent of EGFR/Shc coprecipitation was assessed by EGFR immunoprecipitation/Shc immunoblotting ($n = 2$) (*A,* representative blot) or Shc immunoprecipitation/phosphotyrosine immunoblotting ($n = 1$). *B,* relationship to receptor activation. *x* axis values are from Fig. 3 (mean ± S.E.), and *y* axis values are mean ± S.E., $n = 3$. ◇, no ligand before or after acid wash. ○, pretreatment with TGFα; all *closed symbols,* pretreatment with EGF. ▼, preincubation with 0.1% Me_2SO only; ●, preincubation with 50 μM PD098059.

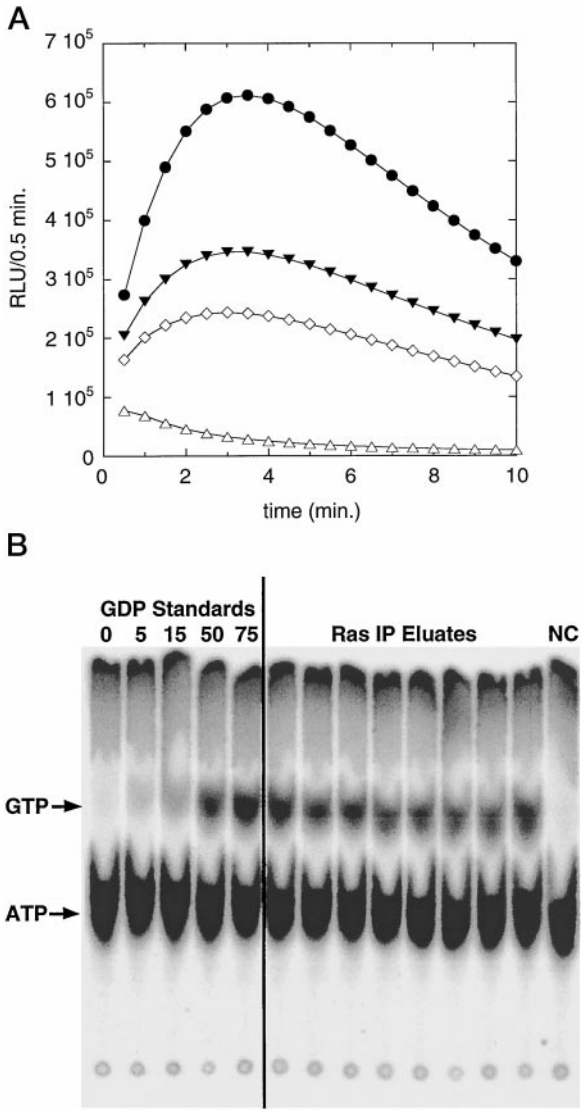

FIG. 7. **Quantitation of GTP and GDP eluted from Ras immunoprecipitates.** *A,* GTP determination. GTP was converted to GDP and ATP by NDP kinase in the presence of excess ADP, and ATP was consumed by firefly luciferase to produce light. The progress of the coupled enzymatic reaction was monitored in a photon-counting luminometer. Shown are representative samples corresponding to cells treated according to the surface titration protocol. ◇, PD098059 preincubation, no ligand stimulation before or after acid wash. ●, PD098059, EGF pretreatment, 20 nM TGFα chase. ▼, same as ● but PD098059 was omitted. △, same as ● but Y13-259 antibody was omitted from the immunoprecipitation. *B,* GDP determination. GDP was converted to radioactive GTP by NDP kinase, using [γ-^{32}P]ATP as the phosphate donor. GTP and ATP were separated by TLC, and the radioactive spots were visualized using a molecular imager. GDP standards, with the initial amount of GDP in fmol indicated, and eluates of Ras immunoprecipitations are shown. The negative control (*NC*) was maximal cell stimulation conditions and omission of Y13-259 antibody in the immunoprecipitation.

of EGFR/Shc coprecipitation (averaged over all three experiments) and EGFR activation was determined by again plotting the variables for each experimental condition, with Tyr(P)-EGFR on the *x* axis (Fig. 6*B*). Because the surface titration protocol was used, the results indicate that coprecipitation is not affected by EGFR trafficking, because points for EGF- and TGFα-pretreated cells fall on the same curve. PD098059 treatment also had no effect on the complexation of Shc with activated EGFR (Fig. 6*B*), again consistent with the nature of the proposed MEK-dependent feedback loop.

Activated EGFR in Internal Compartments Participate in the Activation of Ras—We have established that the ability of the EGFR to elicit membrane recruitment and tyrosine phosphorylation of Shc is not affected by the subcellular location of the activated receptor. However, Shc-dependent activation of Ras could still depend on compartmentalization of the EGFR if the membranes of internal trafficking compartments contained two-dimensional concentrations of Ras that differed from that of the plasma membrane. To ascertain whether generation of Ras-GTP in intact cells is affected by EGFR internalization, the surface titration protocol was again employed, in conjunction with quantitative measurements of the GTP/GDP ratio from immunoprecipitated Ras. To accomplish the latter, assays described by Scheele *et al.* (36) were used that independently assess fmol quantities of GTP and GDP.

GTP was quantified using a kinetic, coupled enzyme assay in which GTP is converted to ATP by NDP kinase in the presence of excess ADP, and ATP is consumed by firefly luciferase in the presence of luciferin to produce light. Measurements using GTP standards confirmed that the kinetics of the reaction were quantitatively consistent with first order conversion of GTP to ATP and first order consumption of ATP. Consistent with that mechanism, integrated photon counts were proportional to the initial amount of GTP in the sample, and the assay could detect as little as 1 fmol of GTP (data not shown). Representative kinetic results for surface titration samples are shown in Fig. 7*A*. Control samples in which Y13-259 antibody was omitted from the immunoprecipitation exhibited much lower photon counts and single exponential decay of reaction rate with time, consistent with the absence of GTP (Fig. 7*A*), as did samples in

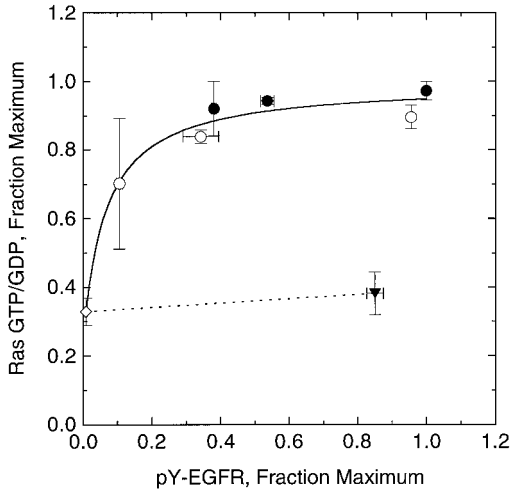

FIG. 8. **Participation of surface and internal EGFR in the activation of Ras.** Cells were treated according to the surface titration protocol, and the ratio of GTP to GDP eluted from Ras immunoprecipitates was determined using methods described in Fig. 7 and under "Experimental Procedures." The results are plotted as a function of total receptor activation. *x* axis values are from Fig. 3 (mean ± S.E.), and *y* axis values are mean ± S.E. ($n = 2$). ◇, no ligand before or after acid wash. ○, pretreatment with TGFα; all *closed symbols,* pretreatment with EGF. ▼, preincubation with 0.1% Me_2SO only; ●, preincubation with 50 μM PD098059.

which NDP kinase was excluded from the reaction mixture (data not shown).

GDP was quantified by conversion to radioactive GTP by NDP kinase in a reaction that was allowed to come to equilibrium, using [γ-^{32}P]ATP as the phosphate donor. GTP and ATP were then separated by thin layer chromatography. Fig. 7*B* shows a phosphorimage of a typical TLC plate spotted with reacted GDP standards and eluates of Ras immunoprecipitates. For the amounts of ATP added to the reactions, standard curves of fractional conversion *versus* fmol of GDP were linear up to 100 fmol of GDP. Control samples in which Y13-259 antibody was omitted from the immunoprecipitation yielded no conversion to [γ-^{32}P]GTP. Based on experiments using GTP and GDP standards, it was estimated that there are approximately 20,000 Ras molecules per NR6 WT cell, in agreement with the amount reported for NIH 3T3 fibroblasts; however, roughly 10% of the Ras molecules were GTP-bound in quiesced NR6 WT cells, over 1 order of magnitude higher than in NIH 3T3 cells (36).

The quantitative relationship between Ras activation, expressed as the ratio of GTP/GDP eluted from cellular Ras, and autophosphorylation of EGFR in surface titration experiments was elucidated by the plot shown in Fig. 8. Activation of Ras at maximal EGFR stimulation correlated quantitatively with the GTP loading experiment described in Fig. 2. Without inhibition of MEK activation, both the level of Ras-GTP and the rate of Ras GNP exchange desensitized to near basal levels by 20 min, whereas PD098059 treatment yielded Ras GTP/GDP and GNP exchange of about 2.8 times the basal level. This is consistent with a Ras activation mechanism in which exchange of GDP for GTP is enhanced, whereas acceleration of GTPase activity is relatively unaffected. As noted for the tyrosine phosphorylation of Shc, the activation of Ras was saturable with respect to Tyr(P)-EGFR and, importantly, did not seem to depend on compartmentalization of the EGFR. Although EGF-pretreated cells exhibited a higher level of Ras-GTP relative to TGFα-pretreated cells, which would be consistent with even more efficient activation of Ras elicited by internal receptors compared with surface receptors, the difference was not statistically significant. It was also confirmed that the saturability of Ras-GTP reflected the true equilibrium relationship at submaximal EGFR activation and not a slow decay after acid washing; PD098059-treated cells stimulated for 20 min with 0.5, 2, or 20 nM EGFR (26, 66, and 100% EGFR activation, respectively) exhibited similar increases in Ras-GTP above the basal level (data not shown).

DISCUSSION

The importance of endocytosis and intracellular sorting in controlling cell growth and transformation mediated by erbB family receptors has been demonstrated in numerous studies, including many using EGFR-expressing NR6 fibroblasts (33, 43–46). However, the regulation of signal transduction via receptor trafficking is complex, because it is not obvious whether signaling ceases immediately after internalization or whether it continues while receptor-ligand complexes remain intact in early endosomes (7). We demonstrated previously that EGFR-mediated PLC-γ1 signaling does not occur in intracellular compartments of NR6 cells, despite continued tyrosine phosphorylation of EGFR and PLC-γ1. This is probably because the membrane lipid target of the pathway phosphatidylinositol (4,5)-bisphosphate (PIP_2) is compartmentalized (32). To extend this area of research, we examined the possible effects of subcellular location on the activation of Ras, another membrane-associated intermediate involved in EGFR signaling.

In fibroblasts, the primary linkage between EGFR and Ras activation is achieved through the tyrosine phosphorylation of Shc. In cells expressing variant EGFR that lack autophosphorylation sites, efficient tyrosine phosphorylation of Shc, activation of the Ras/Erk pathway, and stimulation of mitogenesis are still observed in response to EGF (47, 48). This initially suggested that Shc phosphorylation and subsequent formation of Shc·Grb2·Sos complexes are sufficient for increased Ras-GNP exchange. However, three lines of evidence suggest that membrane localization of Shc·Grb2·Sos complexes is also important. First, because Ras is laterally mobile in cellular membranes (49), recruitment of Ras-GEF activity to the membrane would theoretically enhance its association with Ras by at least 100–1000-fold (50). Second, ligation of the kinase-positive, autophosphorylation-negative c′973 truncated EGFR still stimulates membrane recruitment of *in vitro* Ras-GEF activity, as well as tyrosine phosphorylation of erbB-2, in NR6 cells (38). Finally, whereas EGF elicits Shc phosphorylation, localization of Shc to the plasma membrane, and the downstream activation of Erk in NR6 cells expressing an active EGFR/erbB-2 chimera, EGF stimulates efficient tyrosine phosphorylation of Shc but fails to induce membrane recruitment of Shc or Erk activation in NR6 cells expressing a kinase-positive, autophosphorylation-negative chimera (31). This last result also suggests that tyrosine phosphorylation of receptors is at least permissive for, if not directly mediating, Shc recruitment. It is also known that EGF treatment can induce recruitment of Shc to endosomal membranes (30, 31), presumably mediated by internalized EGF·EGFR complexes. In rat liver, the time course of Shc recruitment to endosomal membranes parallels that of internal EGFR autophosphorylation, and the endosome-associated Shc is efficiently tyrosine phosphorylated (30).

By exploiting the different affinities of EGF and TGFα for the EGFR in endosomes, we demonstrated that autophosphorylated EGFR at the surface and in internal compartments of NR6 WT cells are equal in their ability to form a complex with Shc and, presumably, localize Shc to membranes *in vivo*. Tyrosine phosphorylation of Shc was also not dependent on the surface:internal ratio of activated receptors. Compared with the apparent extent of Shc binding to activated receptors, how-

ever, the level of total tyrosine-phosphorylated Shc was relatively insensitive to EGFR activation (compare Figs. 5*B* and 6*B*). This result can be explained using a fairly simple mathematical expression relating the fraction of total cellular Shc that is tyrosine-phosphorylated to the fraction that is in complex with the receptor (see "Appendix"). The observed results are consistent with Shc remaining tyrosine-phosphorylated after dissociation from the EGFR, with the fraction of total phosphorylated Shc being determined by the equilibrium between kinase and phosphatase activities at cellular membranes.

We also investigated the generation of Ras-GTP, because the constitutive membrane localization of Ras might affect its accessibility to plasma membrane- and endosome-associated GEF activity. On the time scale of EGFR trafficking, Ras activation in NR6 WT was desensitized by a MEK-dependent negative feedback loop. This attenuation mechanism, which can be blocked by using the MEK-specific inhibitor PD098059, has been reported to disrupt Shc·Grb2·Sos complexes. Consistent with this mode of action, the upstream events of EGFR/Shc complexation and Shc phosphorylation were not affected by MEK activation. As with Shc phosphorylation, there was an insensitive relationship between stimulation of Ras-GTP and total receptor activation when cells were treated with PD098059. The level of Ras-GTP did not significantly depend on the localization of activated receptors, and certainly, internal receptors were no less efficient than surface receptors in contributing to generation of Ras-GTP. This is in direct opposition to PIP_2 hydrolysis by phospholipase C in the same cell line, which is ablated by EGFR endocytosis.

Two conceptual models adequately explain our Ras-GTP results, as illustrated in Fig. 9. In the first (Fig. 9*A*), Sos is recruited to both the plasma membrane and internal membranes, where Ras is activated. To be quantitatively consistent with our data, the different cellular membranes would have to contain, on average, roughly equal concentrations of Ras. The main feature of this mechanism is that with respect to this pathway, the plasma membrane and endosomal membrane environments are equivalent. In the second model (Fig. 9*B*), Ras-GEF activity simply reflects the total level of Tyr(P)-Shc in the cell, and Ras is activated at the plasma membrane. If membrane localization of Shc·Grb2·Sos complexes is required, then this would be mediated by a mechanism that is insensitive to or independent of EGFR activation. An important feature of this mechanism is that Ras can in principle be deficient or even absent in endosomal membranes, and the contribution of internal EGFR to Ras activation is simply to phosphorylate its fair share of Shc molecules.

Although the latter model invokes more assumptions, a possible molecular basis centers around protein-lipid interactions. Upon formation of a receptor-Shc·Grb2·Sos complex, an interaction between the Sos pleckstrin homology domain and a specific membrane lipid would be stabilized by analogy to the effect of Sos localization on its association with Ras-GDP. This complex might then allow the Shc phosphotyrosine-binding domain to rapidly exchange its phosphotyrosine ligand for a lipid (51), generating an assembly that could exist transiently as an independent species. The Sos pleckstrin homology domain and Shc phosphotyrosine-binding domain both bind PIP_2 *in vitro* (52, 53), and our previous results suggest that activated EGFR only has access to this lipid at the plasma membrane. Also, both PIP_2 and Ras have been found to be concentrated in low buoyant density fractions of plasma membrane preparations (54, 55). Distinguishing between the two conceptual models of Ras activation will require quantitative determinations of the Ras concentrations in the plasma membrane and endosomal membranes. By immunofluorescence, wild-type Ras is predominantly seen at the plasma membrane (56); however, fractionation of endosomes suggests the presence of Ras (57). Indeed, endosomes isolated from EGF-treated A-431 cells can activate Erk in cytosolic preparations from unstimulated cells (58).

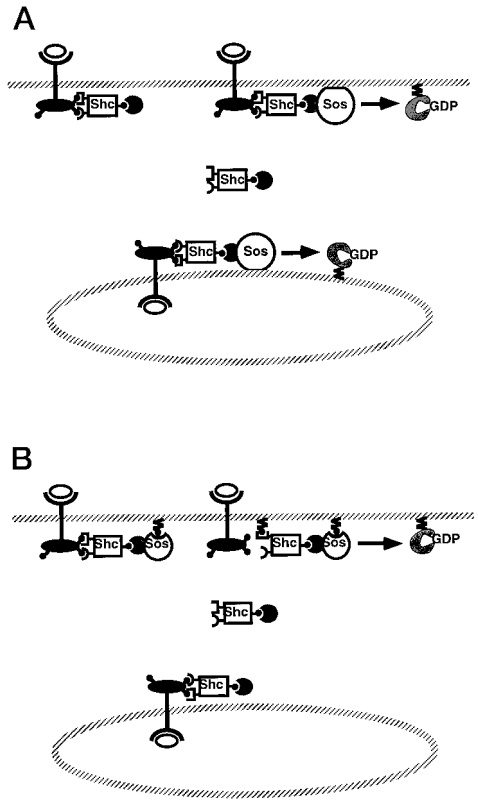

FIG. 9. **Two conceptual models of Ras activation by the EGFR.** *A,* tyrosine phosphorylation of Shc is mediated by both surface and internal EGFR, recruiting Sos to both the plasma membrane and endosomal membranes, where it encounters Ras at roughly equal concentrations. *B,* tyrosine phosphorylation of Shc is mediated by both surface and internal EGFR, but recruitment of associated Sos is only stabilized at the plasma membrane. Stabilization would likely depend on lipid interactions with the pleckstrin homology domain of Sos and/or the phosphotyrosine-binding domain of Shc.

Receptors in complex with cytosolic proteins almost invariably target membrane-associated molecules, including PIP_2 and other membrane lipids, Ras and related small GTPases, heterotrimeric G-proteins, and Src family tyrosine kinases, to carry out signaling functions. Based on theoretical as well as experimental work, we assert that the membrane localization of these molecules affects the organization of signaling interactions in two major ways: 1) it allows amplification of signaling via recruitment of enzymes from the cytosol to the membrane, which is expected to completely synergize with allosteric effects and covalent modifications like phosphorylation, and 2) it allows variations in component concentrations and formation of microdomains to arise based on the chemical interactions between different membrane lipids. The latter would also affect the composition of endosomes relative to the plasma membrane, environments that are physically separated. For these reasons, models of intracellular signal transduction pathways that do not account for cellular structure are likely to be inadequate.

Compartmentalization of various membrane-associated target molecules would allow cells to employ receptor endocytosis as a means to shut off certain signaling pathways in a selective manner. We have demonstrated the feasibility of this hypothesis by showing that EGFR-stimulated hydrolysis of PIP_2 by

PLC-γ1 is restricted to the plasma membrane, whereas the EGFR in internal compartments also participates in the activation of Ras in the same cell line. The PLC pathway, but not the Ras pathway, is therefore regulated locally by removing receptors from their point of action. To rapidly deactivate Ras and therefore regulate cell responses, the cell instead uses a desensitization mechanism that presumably acts in a global fashion to disassemble Shc·Grb2·Sos complexes. This feedback loop can be short-circuited by activating mutations in Ras, leading to uncontrolled cell growth if such mutations go unchecked. The differential regulation of the PLC and Ras pathways is suggestive of their distinct roles in cell functions triggered by pleiotropic signaling recepors. In fibroblasts, activation of PLC-γ1 and hydrolysis of PIP_2 are dispensable for mitogenesis and instead enhance cell motility by releasing actin-modifying proteins into the cytosol (11, 59). Based on the nature of actin dynamics, this mechanism is expected to affect the cytoskeleton locally. On the other hand, activation of the Ras/Erk pathway is a requirement for mitogenesis in fibroblasts but it is also a requirement for EGFR-mediated cell motility. However, the Ras/Erk pathway affects cell migration globally by stimulating the dissociation of focal contacts with the substratum (13). It is therefore tempting to speculate that these divergent signaling pathways differ in their abilities to provide the cell with spatial information regarding its surroundings, a distinction reflected in how these pathways are activated and regulated.

Acknowledgments—We gratefully acknowledge Michael Lässle, Anand Asthagiri, and Gargi Maheshwari at Massachusetts Institute of Technology and Gerry Boss at University of California at San Diego for helpful discussions.

APPENDIX

In this paper, the extents of Shc tyrosine phosphorylation and EGFR/Shc coprecipitation were assessed under conditions that manipulated the magnitude and subcellular locations of EGFR tyrosine autophosphorylation (Figs. 5 and 6, respectively). We were able to conclude that tyrosine phosphorylation of Shc and EGFR/Shc complexation are not dependent on the localization of active receptors. However, the levels of Tyr(P)-Shc and EGFR/Shc coprecipitation exhibited differing sensitivities to changes in total Tyr(P)-EGFR (compare Figs. 5*B* and 6*B*). The level of Tyr(P)-Shc reached a maximum at a significantly lower level of Tyr(P)-EGFR, despite the fact that only about 10% of the total Shc was tyrosine-phosphorylated. Assuming that EGFR/Shc coprecipitation is quantitatively indicative of EGFR/Shc complex formation *in vivo*, we wanted to address whether this observation is reasonable and what mechanistic insights we might infer from it.

Previously, a mathematical model was formulated that relates the association of a cytosolic protein (*e.g.* Shc) with the receptor, and the tyrosine phosphorylation of the protein at cellular membranes, to the numbers of active, autophosphorylated receptors at the cell surface and at intracellular locations (60). The major assumptions of the model were that the cytosolic protein does not compete with other proteins for binding sites on the receptor, that the protein can only be phosphorylated when in complex with the receptor, and that the system achieves a pseudo-steady state on the experimental time scale.

Analysis of the model demonstrated that, for typical cellular parameters, transport of molecules in the cytosol by diffusive processes is relatively rapid, such that the cytosol is homogeneous with respect to the phosphorylated protein of interest. Given also that surface and internal receptors are equal in their ability to bind and phosphorylate Shc in the cell type of interest, we do not need to distinguish receptor pools in different cellular compartments to model signal transduction at this level. These additional stipulations greatly simplify the model equations.

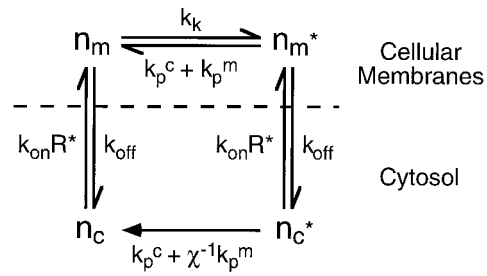

FIG. 10. **Simplified mathematical model of receptor-mediated Binding and phosphorylation of intracellular substrates.** Unphosphorylated and phosphorylated substrate in the cytosol (n_C and n_C^*, respectively) reversibly associate with activated receptors free for binding (R^*), mediating recruitment to cellular membranes. Membrane-associated substrate in the unphosphorylated state (n_m) is phosphorylated by a first order mechanism (rate constant, k_k), and membrane-associated substrate in the phosphorylated state (n_m^*) is dephosphorylated by both cytosolic and membrane-associated phosphatases (observed rate constants, k_p^C and k_p^m, respectively). Substrate in the cytosol can also be dephosphorylated, but the contribution of membrane phosphatases is significantly diminished by the geometric factor χ.

A schematic of the model state transitions, with relevant rate constants, is illustrated in Fig. 10. n_C^* and n_C are the fractions of the protein of interest that are phosphorylated and unphosphorylated, respectively, and located in the cytosol. n_m^* and n_m are the fractions of the protein that are phosphorylated and unphosphorylated, respectively, and associated with cellular membranes. The phosphorylation stoichiometry of the protein in the cytosol is given by the following equation,

$$\frac{n_c^*}{n_C^* + n_C} = \frac{\phi Q n_b}{Q n_b + (\delta_p^C + \chi^{-1}\delta_p^m)(1 - n_b)}$$
$$\phi \equiv \frac{k_k}{k_k + k_p^m + k_p^C}; Q \equiv \frac{k_k + k_p^m + k_p^C}{k_{off} + k_k + k_p^m + k_p^C}; \delta_p^i \equiv \frac{k_p^i}{k_{off}} \quad \text{(Eq. 1)}$$

where n_b is the fraction of the protein that is bound to receptors ($n_b = n_m^* + n_m$). The parameter ϕ describes the balance of kinase and phosphatase activities that act upon the protein at cellular membranes, and Q is an exchange parameter related to the average number of covalent modifications the protein undergoes during an encounter with a receptor (60). The geometric factor χ accounts for the fact that membrane-associated phosphatases would dephosphorylate membrane-associated proteins much more efficiently than they would proteins in the cytosol (50). For the phosphorylation stoichiometry of membrane-associated protein, the following relationship is easily shown.

$$\frac{n_m^*}{n_m^* + n_m} = (1 - Q)\left(\frac{n_C^*}{n_C^* + n_C}\right) + \phi Q \quad \text{(Eq. 2)}$$

Thus, the exchange parameter Q determines the extent of "mixing" between the cytosol and membrane compartments. The total level of phosphoprotein is given by the following equation,

$$n_T^* \equiv n_C^* + n_m^* = \phi\left[\frac{(1 - Q n_b)Q n_b}{Q n_b + (\delta_p^C + \chi^{-1}\delta_p^m)(1 - n_b)} + Q n_b\right] \quad \text{(Eq. 3)}$$

and so there is a direct relationship between protein phosphorylation (n_T^*) and protein-receptor binding (n_b) that is not necessarily a simple proportionality.

The quantitative relationship between the two variables can be characterized by an average sensitivity coefficient, $\bar{\sigma}$.

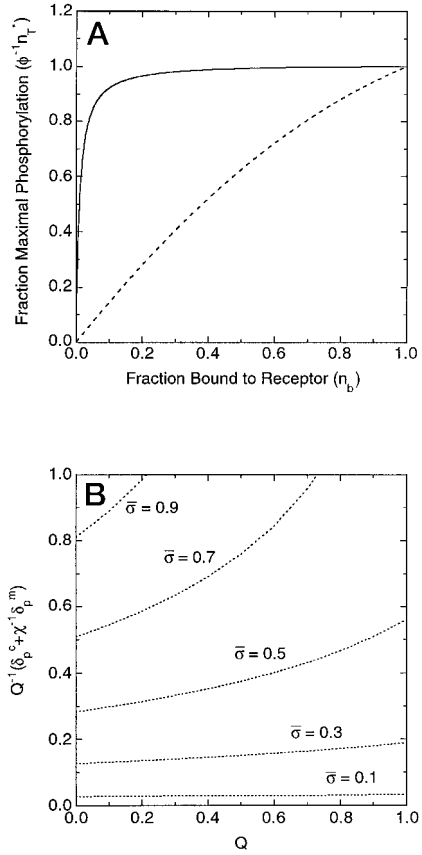

FIG. 11. **Sensitivity of substrate tyrosine phosphorylation relative to formation of receptor-substrate complexes.** *A,* plot of total, normalized tyrosine-phosphorylated substrate ($\phi^{-1}n_T^*$) *versus* the fraction of substrate bound to receptors (n_b), as calculated from Equation 3. The constant parameters are $Q = 0.5$, and $Q^{-1}(\delta_p^C + \chi^{-1}\delta_p^m)$ equal to 0.01 ($\bar{\sigma}$= 0.04) (*solid line*) or 1 ($\bar{\sigma}$ = 0.78) (*dashed line*). *B,* curves of constant $\bar{\sigma}$ in (Q, $Q^{-1}(\delta_p^C + \chi^{-1}\delta_p^m)$) parameter space. $\bar{\sigma}$ is an average sensitivity coefficient describing the relationship between n_T^* and n_b, as defined by Equation 4. For $\bar{\sigma} \ll 1$, $\bar{\sigma}$ is a function of $Q^{-1}(\delta_p^C + \chi^{-1}\delta_p^m)$ only, as predicted from Equation 5.

$$\sigma \equiv \left(\frac{n_b}{n_T^*}\right)\frac{dn_T^*}{dn_b};\ \bar{\sigma} \equiv \int_0^1 \sigma dn_b \qquad \text{(Eq. 4)}$$

For example, if n_T^* is proportional to n_b, then $\bar{\boldsymbol{\sigma}} = 1$. If n_T^* is insensitive to n_b, then $\bar{\boldsymbol{\sigma}} \ll 1$. The value of $\bar{\boldsymbol{\sigma}}$ is a function of two quantities: the exchange parameter Q and $\delta_p^C + \chi^{-1}\delta_p^m$. The latter characterizes the dephosphorylation of protein located in the cytosol. As shown in Fig. 11, protein phosphorylation can indeed be much less sensitive than protein-receptor binding in response to increased activation of receptors ($\bar{\boldsymbol{\sigma}} \ll 1$). This requires that the quantity $Q^{-1}(\delta_p^C + \chi^{-1}\delta_p^m)$ be sufficiently low.

$$\lim_{\bar{\sigma}\to 0} \bar{\sigma} = -\left[\frac{Q^{-1}(\delta_p^C + \chi^{-1}\delta_p^m)}{1 - Q^{-1}(\delta_p^C + \chi^{-1}\delta_p^m)}\right]\ln[Q^{-1}(\delta_p^C + \chi^{-1}\delta_p^m)] \qquad \text{(Eq. 5)}$$

Mechanistically, this means that in order for the observed Tyr(P)-Shc and EGFR/Shc coprecipitation data to be quantitatively consistent, Shc-specific protein-tyrosine phosphatases located in the cytosol must be relatively weak in activity, such that tyrosine-phosphorylated Shc persists in the cytosol after dissociation from the receptor. Accumulation of tyrosine-phosphorylated Shc in the cytosol of rat liver cells has been reported, and it was speculated that this pool could participate in activating Ras at the plasma membrane (30). This is implicitly a global model of signal transduction, which we show here to be highly dependent on the relative influences of cytosolic and membrane-associated Shc-tyrosine phosphatases. It should be noted that the data are quantitatively inconsistent with a model in which second order transphosphorylation of receptor-bound Shc by neighboring receptors is significant (60).

On the other hand, if a cytosolic protein is efficiently dephosphorylated after it dissociates from a receptor complex ($Q^{-1}(\delta_p^C + \chi^{-1}\delta_p^m)$ on the order of 1 or greater), then only receptor-bound proteins can be phosphorylated ($\bar{\boldsymbol{\sigma}} = 1$). If $n_b \ll 1$, then it can be shown that n_T^* would be proportional to the level of Tyr(P)-EGFR in this case, which is exactly what we observed for the EGFR-mediated phosphorylation of PLC-γ1 (32).

Note Added in Proof—It has also been recently observed that tyrosine phosphorylation of PLCγ parallels EGFR activation in rat hepatocytes and that the portion of PLCγ recruited to the particulate fraction is small yet highly phosphorylated relative to the cytosolic fraction (Kholodenko, B. N., Demin, O. V., Moehren, G., and Hoek, J. B. (1999) *J. Biol. Chem.* **274,** 30169–30181). This is consistent with our analysis, although this result was interpreted differently by the investigators.

REFERENCES

1. van der Geer, P., Hunter, T., and Lindberg, R. A. (1994) *Annu. Rev. Cell Biol.* **10,** 251–337
2. Lemmon, M. A., and Schlessinger, J. (1994) *Trends Biochem. Sci.* **19,** 459–463
3. Rosenthal, A., Lindquist, P. B., Bringman, T. S., Goeddel, D. V., and Derynck, R. (1986) *Cell* **46,** 301–309
4. Ouyang, X. M., Gulliford, T., Huang, G. C., and Epstein, R. J. (1999) *J. Cell. Physiol.* **179,** 52–57
5. Ebner, R., and Derynck, R. (1991) *Cell Regul.* **2,** 599–612
6. French, A. R., Tadaki, D. K., Niyogi, S. K., and Lauffenburger, D. A. (1995) *J. Biol. Chem.* **270,** 4334–4340
7. Baass, P. C., Di Guglielmo, G. M., Authier, F., Posner, B. I., and Bergeron, J. J. M. (1995) *Trends Cell Biol.* **5,** 465–470
8. Bos, J. L. (1989) *Cancer Res.* **49,** 4682–4689
9. Bourne, H. R., Sanders, D. A., and McCormick, F. (1991) *Nature* **349,** 117–127
10. Vojtek, A. B., and Der, C. J. (1998) *J. Biol. Chem.* **273,** 19925–19928
11. Chen, P., Xie, H., Sekar, M. C., Gupta, K., and Wells, A. (1994) *J. Cell Biol.* **127,** 847–857
12. Klemke, R. L., Cai, S., Giannini, A. L., Gallagher, P. J., de Lanerolle, P., and Cheresh, D. A. (1997) *J. Cell Biol.* **137,** 481–492
13. Xie, H., Pallero, A., Gupta, K., Ware, M. F., Chang, P., Witke, W., Kwiatkowski, D. J., Lauffenburger, D. A., Murphy-Illrich, J. E., and Wells, A. (1998) *J. Cell Sci.* **111,** 616–625
14. Aronheim, A., Engelberg, D., Li, N., Al-Alawi, N., Schlessinger, J., and Karin, M. (1994) *Cell* **78,** 949–961
15. Quilliam, L. A., Huff, S. Y., Rabun, K. M., Wei, W., Park, W., Broek, D., and Der, C. J. (1994) *Proc. Natl. Acad. Sci. U. S. A.* **91,** 8512–8516
16. Buday, L., and Downward, J. (1993) *Cell* **73,** 611–620
17. Cussac, D., Frech, M., and Chardin, P. (1994) *EMBO J.* **13,** 4011–4021
18. Pawson, T. (1995) *Nature* **373,** 573–580
19. Downward, J., Parker, P., and Waterfield, M. D. (1984) *Nature* **311,** 483–485
20. Batzer, A. G., Rotin, D., Urena, J. M., Skolnik, E. Y., and Schlessinger, J. (1994) *Mol. Cell. Biol.* **14,** 5192–5201
21. Okabayashi, Y., Kido, Y., Okutani, T., Sugimoto, Y., Sakaguchi, K., and Kasuga, M. (1994) *J. Biol. Chem.* **269,** 18674–18678
22. Sasaoka, T., Langlois, W. J., Leitner, J. W., Draznin, B., and Olefsky, J. M. (1994) *J. Biol. Chem.* **269,** 32621–32625
23. de Vries-Smits, A. M. M., Pronk, G. J., Medema, J. P., Burgering, B. M. T., and Bos, J. L. (1995) *Oncogene* **10,** 919–925
24. Langlois, W. J., Sasaoka, T., Saltiel, A. R., and Olefsky, J. M. (1995) *J. Biol. Chem.* **270,** 25320–25323
25. Rozakis-Adcock, M., van der Geer, P., Mbamalu, G., and Pawson, T. (1995) *Oncogene* **11,** 1417–1426
26. Porfiri, E., and McCormick, F. (1996) *J. Biol. Chem.* **271,** 5871–5877
27. Holt, K. H., Waters, S. B., Okada, S., Yamauchi, K., Decker, S. J., Saltiel, A. R., Motto, D. G., Koretsky, G. A., and Pessin, J. E. (1996) *J. Biol. Chem.* **271,** 8300–8306
28. Osterop, A. P. R. M., Medema, R. H., van der Zon, G. C. M., Bos, J. L., Moller, W., and Maassen, J. A. (1993) *Eur. J. Biochem.* **212,** 477–482
29. Klarlund, J. K., Cherniak, A. D., and Czech, M. P. (1995) *J. Biol. Chem* **270,** 23421–23428
30. Di Guglielmo, G. M., Baass, P. C., Ou, W., Posner, B. I., and Bergeron, J. J. M. (1994) *EMBO J.* **13,** 4269–4277
31. Lotti, L. V., Lanfrancone, L., Migliaccio, E., Zompetta, C., Pelicci, G., Salcini, A. E., Falini, B., Pelicci, P. G., and Torrisi, M. R. (1996) *Mol. Cell. Biol.* **16,** 1946–1954
32. Haugh, J. M., Schooler, K., Wells, A., Wiley, H. S., and Lauffenburger, D. A. (1999) *J. Biol. Chem.* **274,** 8958–8965
33. Wells, A., Welsh, J. B., Lazar, C. S., Wiley, H. S., Gill, G. N., and Rosenfeld, M. G. (1990) *Science* **247,** 962–964
34. Alessi, D. R., Cuenda, A., Cohen, P., Dudley, D. T., and Saltiel, A. R. (1995) *J. Biol. Chem.* **270,** 27489–27494
35. de Vries-Smits, A. M. M., van der Voorn, L., Downward, J., and Bos, J. L. (1995) *Methods Enzymol.* **255,** 156–161
36. Scheele, J. S., Rhee, J. M., and Boss, G. R. (1995) *Proc. Natl. Acad. Sci. U. S. A.* **92,** 1097–1100
37. Medema, R. H., De Vries-Smits, A. M. M., Zon, G. C. M., Maassen, J. A., and Bos, J. L. (1993) *Mol. Cell. Biol.* **13,** 155–162

38. Sasaoka, T., Langlois, W. J., Bai, F., Rose, D. W., Leitner, J. W., Decker, S. J., Saltiel, A. R., Gill, G. N., Kobayashi, M., Draznin, B., and Olefsky, J. M. (1996) *J. Biol. Chem.* **271,** 8338–8344
39. Morrison, P., Saltiel, A. R., and Rosner, M. R. (1996) *J. Biol. Chem.* **271,** 12891–12896
40. Lund, K. A., Opresko, L. K., Starbuck, C., Walsh, B. J., and Wiley, H. S. (1990) *J. Biol. Chem.* **265,** 15713–15723
41. Okada, S., Kao, A. W., Ceresa, B. P., Blaikie, P., Margolis, B., and Pessin, J. E. (1997) *J. Biol. Chem.* **272,** 28042–28049
42. Ricci, A., Lanfrancone, L., Chiari, R., Belardo, G., Pertica, C., Natali, P. G., Pelicci, P. G., and Segatto, O. (1995) *Oncogene* **11,** 1519–1529
43. Masui, H., Wells, A., Lazar, C. S., Rosenfeld, M. G., and Gill, G. N. (1991) *Cancer Res.* **51,** 6170–6175
44. Reddy, C. C., Wells, A., and Lauffenburger, D. A. (1994) *Biotechnol. Prog.* **10,** 377–384
45. Lenferink, A. E. G., Pinkas-Kramarski, R., van de Poll, M. L. M., van Vugt, M. J. H., Klapper, L. N., Tzahar, E., Waterman, H., Sela, M., van Zoelen, E. J. J., and Yarden, Y. (1998) *EMBO J.* **17,** 3385–3397
46. Worthylake, R., Opresko, L. K., and Wiley, H. S. (1999) *J. Biol. Chem.* **274,** 8865–8874
47. Gotoh, N., Tojo, A., Muroya, K., Hashimoto, Y., Hattori, S., Nakamura, S., Takenawa, T., Yazaki, Y., and Shibuya, M. (1994) *Proc. Natl. Acad. Sci. U. S. A.* **91,** 167–171
48. Soler, C., Alvarez, C. V., Beguinot, L., and Carpenter, G. (1994) *Oncogene* **9,** 2207–2215
49. Niv, H., Gutman, O., Henis, Y. I., and Kloog, Y. (1999) *J. Biol. Chem.* **274,** 1606–1613
50. Haugh, J. M., and Lauffenburger, D. A. (1997) *Biophys. J.* **72,** 2014–2031
51. Ravichandran, K. S., Zhou, M., Pratt, J. C., Harlan, J. E., Walk, S. F., Fesik, S. W., and Burakoff, S. J. (1997) *Mol. Cell. Biol.* **17,** 5540–5549
52. Kubiseski, T. J., Chook, Y. M., Parris, W. E., Rozakis-Adcock, M., and Pawson, T. (1997) *J. Biol. Chem.* **272,** 1799–1804
53. Zhou, M. M., Ravichandran, K. S., Olejniczak, E. T., Petros, A. M., Meadows, R. P., Sattler, M., Harlan, J. E., Wade, W. S., Burakoff, S. J., and Fesik, S. W. (1995) *Nature* **378,** 584–592
54. Mineo, C., James, G. L., Smart, E. J., and Anderson, R. G. W. (1996) *J. Biol. Chem.* **271,** 11930–11935
55. Pike, L. J., and Casey, L. (1996) *J. Biol. Chem.* **271,** 26453–26456
56. Willumsen, B. M., Cox, A. D., Solski, P. A., Der, C. J., and Buss, J. E. (1996) *Oncogene* **13,** 1901–1909
57. Pol, A., Calvo, M., and Enrich, C. (1998) *FEBS Lett.* **441,** 34–38
58. Xue, L. Z., and Lucocq, J. (1998) *Cell. Signal.* **10,** 339–348
59. Chen, P., Murphy-Ullrich, J. E., and Wells, A. (1996) *J. Cell Biol.* **134,** 689–698
60. Haugh, J. M., and Lauffenburger, D. A. (1998) *J. Theor. Biol.* **195,** 187–218